Acta Crystallographica Section F
Structural Biology and Crystallization Communications
ISSN 1744-3091

Crystallization and preliminary X-ray diffraction analysis of human IL-22 bound to the extracellular IL-22R1 chain

Brandi C. Jones,[a] Naomi J. Logsdon[a] and Mark R. Walter[a,b]*

[a]Center for Biophysical Sciences and Engineering, University of Alabama at Birmingham, Birmingham, AL 35294, USA, and [b]Department of Microbiology, University of Alabama at Birmingham, Birmingham, AL 35294, USA

Correspondence e-mail: walter@uab.edu

Received 19 December 2007
Accepted 18 February 2008

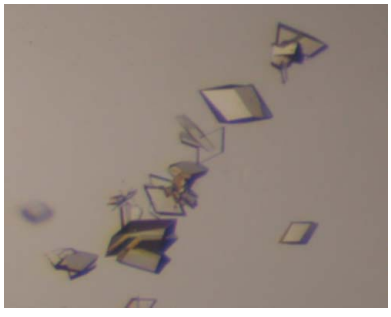

Interleukin-22 (IL-22) is a potent mediator of cellular inflammatory responses. Crystals of IL-22 bound to the extracellular high-affinity cell-surface receptor sIL-22R1 have been grown from polyethylene glycol solutions. Crystals suitable for X-ray diffraction analysis were only obtained with mutants of IL-22 and sIL-22R1 that removed the N-linked glycosylation sites found in the wild-type amino-acid sequences. The crystals belonged to space group $P2_1$, with unit-cell parameters $a = 50.43$, $b = 76.33$, $c = 114.92$ Å, $\beta = 92.45^\circ$, and diffracted X-rays to 3.2 Å resolution. The crystallographic asymmetric unit contained two IL-22–sIL-22R1 complexes, corresponding to a solvent content of approximately 52%.

1. Introduction

Interleukin-22 (IL-22) is an α-helical cytokine produced by activated T cells, including the recently identified Th17 lineage (Dumoutier, Louahed *et al.*, 2000; Xie *et al.*, 2000; Liang *et al.*, 2006; Harrington *et al.*, 2005). IL-22 up-regulates the production of early systemically circulated defense proteins (acute phase proteins) such as serum amyloid A, α1-antichymotrypsin and haptoglobin in liver cells (Dumoutier, Van Roost *et al.*, 2000). In contrast to its pro-inflammatory functions, IL-22 appears to have a protective effect on the liver by promoting hepatocyte survival (Pan *et al.*, 2004; Radaeva *et al.*, 2004; Zenewicz *et al.*, 2007). IL-22 also up-regulates gene expression of pancreatitis-associated protein PAP1 in acinar cells (Aggarwal *et al.*, 2001) and induces the production of reactive oxygen species (ROS) in B-cells (Wei *et al.*, 2003). More recently, IL-22 expression levels have been shown to be elevated in active Crohn's disease and IL-22 has been shown to contribute to the dermal inflammation associated with psoriasis (Zheng *et al.*, 2007; Brand *et al.*, 2006).

IL-22 is a member of the class 2 cytokine family, which includes IL-10, IL-19, IL-20, IL-24, IL-26, IL-28 and IL-29 (Walter, 2002; Fickenscher *et al.*, 2002; Pestka *et al.*, 2004; Langer *et al.*, 2004). IL-22 cellular responses are initiated by the assembly of a cell-surface heterodimeric complex consisting of IL-22R1 and IL-10R2 chains (Xie *et al.*, 2000; Kotenko *et al.*, 2001*a*). IL-22R1 (SWISS-PROT ID Q9HB22) is a 574-amino-acid protein that contains an extracellular ligand-binding domain, a membrane-spanning helix and an intracellular domain (Xie *et al.*, 2000). IL-10R2 (SWISS-PROT ID Q08334) shares a similar organization, but its intracellular domain consists of only ~76 residues, compared with ~320 for IL-22R1 (Kotenko *et al.*, 1997). Although IL-22 is produced by T cells, IL-22R1 is predominantly expressed on skin and mucosal epithelia (Wolk & Sabat, 2006; Nagalakshmi *et al.*, 2004). In contrast, IL-10R2 is expressed on all cell types, which reflects its role as a shared receptor in IL-10, IL-26, IL-28 and IL-29 receptor complexes (Langer *et al.*, 2004). The binding affinities obtained using soluble extracellular IL-22R1 (sIL-22R1) and IL-10R2 (sIL-10R2) chains suggest that complex formation is sequential (Logsdon *et al.*, 2002). For example, IL-22R1 first forms a high-affinity complex with IL-22, followed by relatively weak interactions with the signal-transducing IL-10R2 chain. Formation of the IL-22–IL-22R1–IL-10R2 cell-surface complex activates kinases (JAK1, Tyk2 and MAP kinases)

and transcription factors, especially STAT3, leading to IL-22-specific cellular responses (Lejeune *et al.*, 2002).

The IL-22 amino-acid sequence contains three N-linked glycosylation sites (Asn-*X*-Ser/Thr, where *X* is any amino acid) at Asn54, Asn68 and Asn97 denoted by the convention IL-22$_{NNN}$ (Logsdon *et al.*, 2004). Point mutants of Asn54 (IL22$_{QNN}$ or IL-22$_{ANN}$), but not Asn68 (IL-22$_{NQN}$) or Asn97 (IL-22$_{NNQ}$), disrupt IL-10R2 binding and IL-22 signaling (Logsdon *et al.*, 2004; Wolk *et al.*, 2004). The crystal structures of IL-22 produced in *Escherichia coli* (IL-22$_{Ec}$) as well as glycosylated IL-22 expressed in insect cells have been determined (Nagem *et al.*, 2002; Xu *et al.*, 2005). IL-22 folds into a compact monomeric structure that resembles one subunit of the IL-10 dimer (Walter & Nagabhushan, 1995; Zdanov *et al.*, 1995). Although IL-22 adopts a monomeric structure, recent X-ray scattering data suggest that IL-22 forms dimeric structures similar to IL-10 in solution (de Oliveira Neto *et al.*, 2008). Although crystallographic and other biophysical studies have been performed on IL-22 itself, structural studies on sIL-22R1 or sIL-10R2, alone or in complex with IL-22, have not been reported. Owing to the importance of the IL-22 in human disease, we have initiated structural studies on the complex between IL-22 and sIL-22R1. Here, we report the crystallization of the IL-22–sIL-22R1 complex, which may aid in the understanding of the structural basis for IL-22-mediated cross-talk between the immune system and epithelial cells.

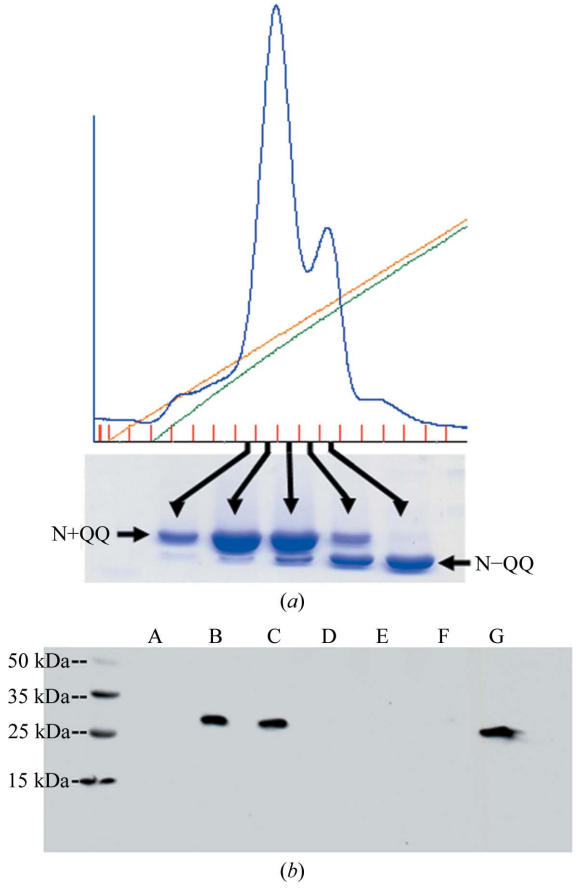

Figure 1
Separation and expression of IL-22 and sIL-22R1 glycosylation variants. (*a*) Anion-exchange chromatogram demonstrating the separation of IL-22$_{N+QQ}$ and IL-22$_{N-QQ}$ and SDS–PAGE gel analysis of IL-22$_{NQQ}$ fractions obtained from the chromatogram. (*b*) Expression analysis of sIL-22R1 mutants. The protein was detected by Western blotting with an anti-His antibody. Gel lanes correspond to N80K, N87K (A), N80D, N87D (B), N80D, N87D, T89Q (C), N80S, N87S (D), N80A, N87A (E), T82A, T89A (F) and sIL-10R1-His$_6$ positive control (G).

2. Materials and methods

2.1. Expression and purification

The expression plasmids pAHF/IL-22$_{NQQ}$ and pMT/sIL-22R1 have previously been described (Logsdon *et al.*, 2002, 2004). IL-22$_{NQQ}$ and sIL-22R1$_{DDQ}$ expressed from these vectors contain N- and C-terminal His$_6$ tags, respectively, that can be removed using encoded factor Xa cleavage sites. Site-directed mutants of pMT/sIL-22R1 glycosylation sites were produced using the QuikChange mutagenesis kit (Stratagene). IL-22$_{NQQ}$ and sIL-22R1$_{DDQ}$ were expressed in insect cells as described previously (Logsdon *et al.*, 2004). Briefly, cells were expanded and induced at a cell density of 5×10^6 cells ml^{-1} in serum-free media (Lonza) containing 20 m*M* L-glutamine by the addition of 0.5 m*M* Cu_2SO_4. After 7 d, the expression media containing IL-22$_{NQQ}$ or sIL-22R1$_{DDQ}$ was clarified by centrifugation followed by dialysis into a binding buffer consisting of 20 m*M* Tris–HCl pH 7.9, 0.5 *M* NaCl and 5.0 m*M* imidazole.

1 l of dialyzed medium containing IL-22$_{NQQ}$ or sIL-22R1$_{DDQ}$ was applied to separate 7.5 ml nickel columns (Novagen) at 277 K. The bound proteins were washed with five column volumes of binding buffer containing 15 m*M* imidazole followed by elution with 1 *M* imidizole. Column fractions containing IL-22$_{NQQ}$ or sIL-22R1$_{DDQ}$ were dialyzed overnight into a factor Xa cleavage buffer containing 20 m*M* Tris–HCl pH 8.0, 1 m*M* EDTA, 100 m*M* NaCl, 3 m*M* $CaCl_2$ and concentrated to 0.5 mg ml^{-1} using Centriprep 10 concentrators (Millipore).

2.2. Factor Xa cleavage and separation of IL-22$_{N-QQ}$ and IL-22$_{N+QQ}$ glycosylation variants

The N-terminal His$_6$ tag on IL-22$_{NQQ}$ was removed by overnight digestion with factor Xa [1:50(*w*:*w*); New England BioLabs]. Digested IL-22$_{NQQ}$ was diluted 1:10 into 20 m*M* PIPES pH 6.5 and loaded onto a 1.67 ml POROS HS20 column (Perseptive Biosystems). IL-22$_{N+QQ}$ (carbohydrate attached at Asn54) and IL-22$_{N-QQ}$ (no carbohydrate at Asn54) glycosylation variants were separated with a 0–1 *M* NaCl gradient in 20 column volumes. Fractions containing IL-22$_{N-QQ}$ and IL-22$_{N+QQ}$ were identified by SDS–PAGE and collected for complex formation with sIL-22R1$_{DDQ}$ (Fig. 1).

2.3. Binary IL-22$_{N-QQ}$–sIL-22R1$_{DDQ}$ complex formation

sIL-22R1$_{DDQ}$ containing the C-terminal His$_6$ tag was mixed with a 15% molar excess of IL-22$_{N-QQ}$ prepared as in §2.2. The sIL-22R1$_{DDQ}$ His$_6$ tag was removed by overnight incubation of the IL-22$_{N-QQ}$–sIL-22R1$_{DDQ}$ complex with factor Xa (1:50 protease:complex ratio). The digested complex was concentrated to 10 mg ml^{-1} using a Centricon 10 (Millipore) and injected onto two Superdex 200 HR10/30 gel-filtration columns (Amersham) connected in series. The complex was eluted at 0.35 ml min^{-1} in 150 m*M* NaCl and 20 m*M* Tris–HCl pH 8.0. Eluted fractions containing IL-22$_{N-QQ}$–sIL-22R1$_{DDQ}$ were re-concentrated to 10 mg ml^{-1} for crystallization.

2.4. Crystallization

All crystallization experiments employed the hanging-drop vapor-diffusion method. The hanging drops (2 µl total volume) contained 1 µl IL-22$_{N-QQ}$–sIL-22R1$_{DDQ}$ complex (10 mg ml^{-1}) in 20 m*M* Tris–HCl pH 8.0, 150 m*M* NaCl and 1 µl reservoir solution consisting of 0.1 *M* $MgCl_2$, 13% polyethylene glycol (PEG) 6000 and 0.1 *M* ADA pH 6.8. Streak-seeding was performed from new drops prepared with a reservoir solution containing 0.1 *M* $MgCl_2$, 11% PEG 6000 and 0.1 *M* ADA pH 6.8 and equilibrated for 5 h. A seed stock was obtained by crushing one or two crystals in 50 µl reservoir solution.

2.5. Data collection

The IL-22$_{N-QQ}$–sIL-22R1$_{DDQ}$ crystals were flash-cooled in a nitrogen stream at 100 K for low-temperature data collection. The crystals were cryopreserved in a solution containing 17% PEG 6000, 0.1 *M* $MgCl_2$, 0.1 *M* ADA pH 6.8 and 15% glycerol. To prevent crystal cracking at the final glycerol concentration, the crystals were serially transferred to solutions containing 17% PEG 6000, 0.1 *M* $MgCl_2$, 0.1 *M* ADA pH 6.8 and 0, 5 and 10% glycerol for 15 min each before final transfer into the 15% glycerol solution.

Diffraction data were collected at the South Eastern Region Collaborative Access Team (SER-CAT) beamline ID-22 at the Advanced Photon Source, Argonne National Laboratory. Data were collected on a MAR 300 CCD detector using a wavelength of 1 Å, an oscillation range of 1° and an exposure time of 1 s. Reflection intensities were indexed, integrated and scaled using *HKL*-2000 (Otwinowski & Minor, 1997).

3. Results and discussion

3.1. Protein expression and purification

The IL-22 mutant IL-22$_{NQQ}$ (see Logsdon *et al.*, 2004) was chosen for crystallization studies of the IL-22–sIL-22R1 complex because two of the three N-linked (N*X*S/T) carbohydrate-attachment sites (Asn68 and Asn97) have been mutated to glutamine. The IL-22 glycosylation site at residue Asn54 was not mutated because it had previously been shown to be important for assembly of the IL-22–IL-22R1–IL-10R2 cell-surface complex (Logsdon *et al.*, 2004). Although IL-22$_{NQQ}$ contains only one N-linked glycosylation site, the mutant is expressed as a mixture of glycosylated (IL-22$_{N+QQ}$) and nonglycosylated (IL-22$_{N-QQ}$) molecules. To remove this heterogeneity, anion-exchange chromatography methods were developed to separate IL-22$_{N+QQ}$ from IL-22$_{N-QQ}$ (Fig. 1*a*).

Numerous crystallization screens were performed with receptor complexes containing IL-22$_{N-QQ}$ and sIL-22R1, which encodes three N-linked (N*X*S/T) glycosylation sites at Asn80, Asn87 and Asn172. Complexes were also formed between sIL-22R1 and *E. coli*-produced IL-22 that was refolded from inclusion bodies. However, no crystals or crystallization leads were obtained from any of these IL-22–sIL-22R1 complexes. These results suggested that the glycosylation present on sIL-22R1 may disrupt potential lattice interactions, as previously described for the related IL-10–sIL-10R1 complex (Josephson *et al.*, 2001).

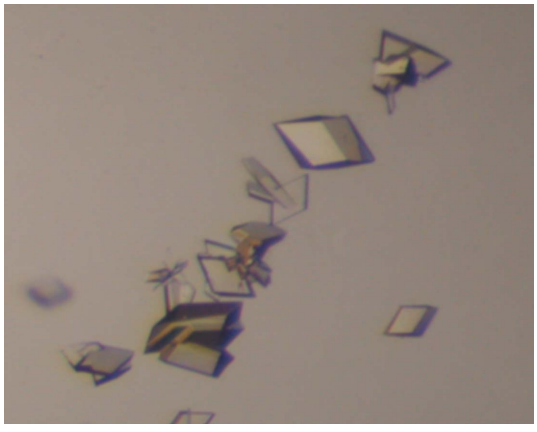

Figure 2
Crystals of IL-22$_{N-QQ}$–sIL-22R1$_{DDQ}$ obtained by streak-seeding.

Table 1
Data-collection statistics.

Values in parentheses are for the highest resolution shell.

Space group	$P2_1$
Resolution (Å)	50–3.2
No. of observations	44091
No. of unique observations	13969
Redundancy	3.2 (2.6)
Completeness (%)	95.6 (93.7)
R_{merge}	0.055 (0.40)
$I/\sigma(I)$	22.4 (2.2)
Unit-cell parameters	
a (Å)	50.43
b (Å)	76.33
c (Å)	114.92
β (°)	92.45

To remove N-linked glycosylation from sIL-22R1, the three asparagines involved in carbohydrate attachment (Asn80, Asn87 and Asn172) were mutated to glutamine. However, no protein was expressed for this sIL-22R1 triple mutant. To overcome this problem, a variety of double mutants that converted sIL-22R1 Asn80 and Asn87 to lysines (*e.g.* Lys80, Lys87), aspartic acids, serines or alanines was performed. Asn172, which corresponds to the third N-linked glycosylation site in sIL-22R1, was left unchanged in these experiments. Small-scale expression analysis revealed that only the aspartic acid double mutant was expressed in insect cells (Fig. 1*b*). Interestingly, sequence alignment of sIL-22R1 and IL-22BP (SWISS-PROT ID Q969J5-2; Dumoutier *et al.*, 2001; Kotenko *et al.*, 2001*b*) revealed that sIL-22R1 residues Asn80 and Asn87 are aspartic acid residues in IL-22BP. Further analysis of the IL-22BP sequence revealed Thr89 in sIL-22R1 to be a glutamine in IL-22BP. To mimic the glycosylation site observed in IL-22BP, the triple mutation sIL-22R1 Asn80Asp, Asn87Asp and Thr89Gln (sIL-22R1$_{DDQ}$) was made and expressed with a yield of 4.5 mg l^{-1} for crystallization studies.

3.2. Crystallization

In contrast to crystallization trials with fully glycosylated sIL-22R1, intergrown thin plates of the IL-22$_{N-QQ}$–sIL-22R1$_{DDQ}$ complex were obtained in 3 d from PEG 6000 solutions containing ADA buffer pH 6.8 at 298 K. To improve the thickness of the crystals, streak-seeding experiments were performed. Specifically, hanging-drop experiments were prepared as before but with a reservoir solution consisting of 0.1 *M* ADA, 0.1 *M* $MgCl_2$, 11% PEG 6000 pH 6.8. After 5 h, streak-seeding was performed using a seed stock made by crushing a single IL-22$_{N-QQ}$–sIL-22R1$_{DDQ}$ plate in 50 µl reservoir solution. After 10 d, diamond-shaped plates with maximal dimensions of 100 × 100 × 55 µm were obtained (Fig. 2).

3.3. X-ray diffraction

Data collection from IL-22$_{N-QQ}$–sIL-22R1$_{DDQ}$ crystals was performed at the APS ID-22 beamline (SER-CAT), which resulted in a complete 3.2 Å resolution data set (Table 1). The *HKL*-2000 indexing routine, combined with an analysis of systematic absences, identified the space group as $P2_1$, with unit-cell parameters a = 50.43, b = 76.33, c = 114.92 Å, β = 92.45°. Gel-filtration analysis reveals that IL-22$_{N-QQ}$–sIL-22R1$_{DDQ}$ is a 1:1 complex with a molecular weight of ∼43 096 Da (Logsdon *et al.*, 2002). Using this molecular weight, solvent estimates of 76% (V_M = 5.1 Å^3 Da^{-1}), 52% (V_M = 2.6 Å^3 Da^{-1}) and 27.5% (V_M = 1.7 Å^3 Da^{-1}) were obtained corresponding to one, two or three 1:1 complexes in the asymmetric unit, respectively (Matthews, 1968). Self-rotation function analysis confirms the presence of a twofold noncrystallographic symmetry axis

in the data. This analysis suggests the crystals contain two 1:1 IL-22_{N-QQ}–sIL-$22R1_{DDQ}$ complexes related by a noncrystallographic twofold axis. This is an interesting result that may allow us to determine whether IL-22 forms an 'IL-10 like' dimeric signaling complex as previously observed in solution (de Oliveira Neto *et al.*, 2008). Phasing of the crystals using molecular replacement and heavy-atom methods is currently under way.

This research was supported by grant AI047300 from the NIH. Use of the Advanced Photon Source was supported by the US Department of Energy, Office of Science, Office of Basic Energy Sciences under Contract No. W-31-109-Eng-38.

References

Aggarwal, S., Xie, M. H., Maruoka, M., Foster, J. & Gurney, A. L. (2001). *J. Interferon Cytokine Res.* **21**, 1047–1053.

Brand, S. *et al.* (2006). *Am. J. Physiol. Gastrointest. Liver Physiol.* **290**, G827–G838.

Dumoutier, L., Lejeune, D., Colau, D. & Renauld, J. C. (2001). *J. Immunol.* **166**, 7090–7095.

Dumoutier, L., Louahed, J. & Renauld, J. C. (2000). *J. Immunol.* **164**, 1814–1819.

Dumoutier, L., Van Roost, E., Colau, D. & Renauld, J. C. (2000). *Proc. Natl Acad. Sci. USA*, **97**, 10144–10149.

Fickenscher, H., Hor, S., Kupers, H., Knappe, A., Wittmann, S. & Sticht, H. (2002). *Trends Immunol.* **23**, 89–96.

Harrington, L. E., Hatton, R. D., Mangan, P. R., Turner, H., Murphy, T. L., Murphy, K. M. & Weaver, C. T. (2005). *Nature Immunol.* **6**, 1123–1132.

Josephson, K., McPherson, D. T. & Walter, M. R. (2001). *Acta Cryst.* D**57**, 1908–1911.

Kotenko, S. V., Izotova, L. S., Mirochnitchenko, O. V., Esterova, E., Dickensheets, H., Donnelly, R. P. & Pestka, S. (2001*a*). *J. Biol. Chem.* **276**, 2725–2732.

Kotenko, S. V., Izotova, L. S., Mirochnitchenko, O. V., Esterova, E., Dickensheets, H., Donnelly, R. P. & Pestka, S. (2001*b*). *J. Immunol.* **166**, 7096–7103.

Kotenko, S. V., Krause, C. D., Izotova, L. S., Pollack, B. P., Wu, W. & Pestka, S. (1997). *EMBO J.* **16**, 5894–5903.

Langer, J. A., Cutrone, E. C. & Kotenko, S. (2004). *Cytokine Growth Factor Rev.* **15**, 33–48.

Lejeune, D., Dumoutier, L., Constantinescu, S., Kruijer, W., Schuringa, J. J. & Renauld, J. C. (2002). *J. Biol. Chem.* **277**, 33676–33682.

Liang, S. C., Tan, X. Y., Luxenberg, D. P., Karim, R., Dunussi-Joannopoulos, K., Collins, M. & Fouser, L. A. (2006). *J. Exp. Med.* **203**, 2271–2279.

Logsdon, N. J., Jones, B. C., Allman, J. C., Izotova, L., Schwartz, B., Pestka, S. & Walter, M. R. (2004). *J. Mol. Biol.* **342**, 503–514.

Logsdon, N. J., Jones, B. C., Josephson, K., Cook, J. & Walter, M. R. (2002). *J. Interferon Cytokine Res.* **22**, 1099–1112.

Matthews, B. W. (1968). *J. Mol. Biol.* **33**, 491–497.

Nagalakshmi, M. L., Murphy, E., McClanahan, T. & de Waal Malefyt, R. (2004). *Int. Immunopharmacol.* **4**, 577–592.

Nagem, R. A., Colau, D., Dumoutier, L., Renauld, J. C., Ogata, C. & Polikarpov, I. (2002). *Structure*, **10**, 1051–1062.

Oliveira Neto, M. de, Ferreira, J. R. Jr, Colau, D., Fischer, H., Nascimento, A. S., Craievich, A. F., Dumoutier, L., Renauld, J. C. & Polikarpov, I. (2008). *Biophys. J.* **94**, 1754–1765.

Otwinowski, Z. & Minor, W. (1997). *Methods Enzymol.* **276**, 307–326.

Pan, H., Hong, F., Radaeva, S. & Gao, B. (2004). *Cell. Mol. Immunol.* **1**, 43–49.

Pestka, S., Krause, C. D., Sarkar, D., Walter, M. R., Shi, Y. & Fisher, P. B. (2004). *Annu. Rev. Immunol.* **22**, 929–979.

Radaeva, S., Sun, R., Pan, H. N., Hong, F. & Gao, B. (2004). *Hepatology*, **39**, 1332–1342.

Walter, M. R. (2002). *Immunol. Res.* **26**, 303–308.

Walter, M. R. & Nagabhushan, T. L. (1995). *Biochemistry*, **34**, 12118–12125.

Wei, C. C., Ho, T. W., Liang, W. G., Chen, G. Y. & Chang, M. S. (2003). *Genes Immun.* **4**, 204–211.

Wolk, K. & Sabat, R. (2006). *Cytokine Growth Factor Rev.* **17**, 367–380.

Wolk, K., Witte, E., Reineke, U., Witte, K., Friedrich, M., Sterry, W., Asadullah, K., Volk, H. D. & Sabat, R. (2004). *Genes Immun.* **5**, 330–336.

Xie, M. H., Aggarwal, S., Ho, W. H., Foster, J., Zhang, Z., Stinson, J., Wood, W. I., Goddard, A. D. & Gurney, A. L. (2000). *J. Biol. Chem.* **275**, 31335–31339.

Xu, T., Logsdon, N. J. & Walter, M. R. (2005). *Acta Cryst.* D**61**, 942–950.

Zdanov, A., Schalk-Hihi, C., Gustchina, A., Tsang, M., Weatherbee, J. & Wlodawer, A. (1995). *Structure*, **3**, 591–601.

Zenewicz, L. A., Yancopoulos, G. D., Valenzuela, D. M., Murphy, A. J., Karow, M. & Flavell, R. A. (2007). *Immunity*, **27**, 647–659.

Zheng, Y., Danilenko, D. M., Valdez, P., Kasman, I., Eastham-Anderson, J., Wu, J. & Ouyang, W. (2007). *Nature (London)*, **445**, 648–651.